Malaysian Journal of Chemistry, 2021, Vol. 23(2), 1-10
(Special Issue: *IKM Pahang Branch Online Symposium 2021 – Chemistry for Sustainable World*)

In Vitro Evaluation of Crosslinked Polyvinyl Alcohol/Chitosan – Gentamicin Sulfate Electrospun Nanofibers

Nazirah Hamdan, Deny Susanti Darnis and Wan Khartini Wan Abdul Khodir*
Department of Chemistry, Kulliyyah of Science, International Islamic University Malaysia Kuantan Campus, Bandar Indera Mahkota, Kuantan 25200, Pahang, Malaysia
*Corresponding author (e-mail: wkhartini@iium.edu.my)

Polymeric nanofibers with good antimicrobial properties are a promising option to thwart wound infection and accelerate wound healing. Although PVA/Chitosan possesses many useful properties, its antibacterial activity is insufficient for effective wound dressing. Therefore, using a hydrophilic drug such as Gentamicin Sulfate (GS) that has a broad-spectrum activity against a wide range of bacteria can enhance the nanofibers' performance. In this study, polyvinyl alcohol (PVA) with chitosan nanofibers loaded with gentamicin sulfate was prepared using an electrospinning technique and crosslinked with glutaraldehyde for better loading efficiency and controlled drug release at the site of interest. Morphological investigation carried out using scanning electron microscopy showed smooth and homogeneous nanofibers. FT-IR was used to confirm the structure of the nanofibers. In situ crosslinking enabled penetration of the crosslinking agent into the nanofibers and improved the thermal stability and drug release performance. The thermal stability of PVA/Chitosan nanofibers was reduced with the addition of gentamicin sulfate. The kinetic release of gentamicin sulfate followed the Korsmeyer-Peppas model with release exponent, $n < 0.5$. Antibacterial testing of crosslinked nanofibers against *Escherichia coli* and *Staphylococcus aureus* showed good inhibition of bacterial growth. Crosslinked PVA/Chitosan nanofibers loaded with gentamicin sulfate showed multifunctional characteristics and thus may be a suitable material for controlled drug delivery and tissue engineering applications.

Key words: Polyvinyl alcohol; chitosan; nanofibers; controlled release

Received: November 2020; Accepted: January 2021

Currently, the development of nanoscale fibers has become a popular choice for drug delivery systems to control the release of drugs to specific sites as it can mimic the native extracellular matrix (ECM) of human skin, and thus promote tissue regeneration and support healing mechanisms. Electrospinning is a promising method commonly used to fabricate nanofibers as it is easy and cost-effective. To produce nanofibers in the electrospinning process, a high voltage power supply is required to introduce a strong potential difference between the polymer solution flowing through a capillary tip and the collector [1].

Polyvinyl alcohol (PVA) is a semi-crystalline synthetic polymer derived from hydrolysis of polyvinyl acetate which has been widely used in biomedical applications [2]. The hydrophilic properties, biocompatibility, biodegradability, excellent thermal stability, nontoxicity, high water permeability, simple processing, good chemical and physical properties of PVA [3] have made it useful in drug delivery systems and medical applications [4].

On the other hand, chitosan is a natural polymer derived from chitin that can be found abundantly in the exoskeletons of crustaceans, insects and molluscs [5]. Chitosan is biodegradable, biocompatible, hydrophilic, nontoxic and has antibacterial properties [6,7] and it is the preferred choice for biomedical applications. It also promotes wound healing by producing fibroblasts, regulating the deposition and arrangement of fibers, facilitating cell migration as well as stimulating granulation and vascularization [8,9,10]. Despite its various advantages, chitosan also shows low chemical strength and a high degradation rate [11]. The addition of chitosan to PVA nanofibers increases the biocompatibility of the nanofibers scaffolds [12]. Moreover, PVA blended with natural polymers such as chitosan, gelatin and collagen can improve the polymeric adhesion of the scaffold [13,14].

Despite its antibacterial properties, chitosan alone is insufficient to treat bacterial infections and heal wounds. Hence, encapsulation of PVA/Chitosan with antibiotics like gentamicin

†Paper presented at the IKM Pahang Branch Online Symposium 2021 – Chemistry for Sustainable World

sulfate can further improve its antibacterial properties against a wide range of bacteria. In addition, it is essential in producing an effective polymeric drug carrier to control and sustain drug release as well as maintain drug stability in the human body. In this study, PVA/Chitosan crosslinked nanofibers encapsulated with gentamicin sulfate were prepared using the electrospinning technique, and its fiber morphology, thermal stability, *in vitro* drug release capability and antibacterial activity were evaluated.

MATERIALS AND METHODS

Materials

Polyvinyl alcohol (viscosity: 45-55 cPs) was purchased from R&M Chemicals (Essex, United Kingdom). Low molecular weight Chitosan (50,000 – 190,000 Da) was purchased from Sigma-Aldrich (Gillingham, UK). Gentamicin sulfate was obtained from Henan Province, China. Acetic acid, Glutaraldehyde and Hydrochloric acid were purchased from Merck (Darmstadt, Germany).

Preparation of PVA/Chitosan Loaded Gentamicin Sulfate Nanofibers.

PVA and chitosan solutions were prepared separately [15]. 10 % (w/v) PVA was dissolved in deionized water and stirred at 50–60 °C while 2.5 % (w/v) Chitosan was dissolved in 2 % v/v aqueous acetic acid solution. Both solutions were left to stir at room temperature for 16 h to ensure homogenization. PVA and chitosan (PC) were combined in a ratio of 85:15 (v/v). Then, gentamicin sulfate was added into the PC solution in three different concentrations: 1 %, 3 % and 5 % (w/v) to produce Gentamicin/PVA/Chitosan (GPC) solution. The solutions were stirred for 30 minutes at room temperature. The GPC nanofibers were fabricated using the electrospinning technique (flow rate: 0.5 ml/h, voltage: 15 kV, distance: 12 cm). The nanofibers obtained were exposed to a mixture of 25 % glutaraldehyde and hydrochloric acid (3:1 v/v) vapor for 6 h for crosslinking. Then the samples were air-dried at room temperature for 24 h to remove the remaining glutaraldehyde and HCl vapour. The crosslinking of nanofibers has been shown to enhance the resistance of nanofibers towards surrounding moisture and prevent rapid degradation of the polymeric nanofibers [16].

Scanning Electron Microscopy (SEM)

The morphology of PC and GPC nanofibers were examined by using SEM (Carl Zeiss S.E Asia/ ZEISS Evo 50). Small sections of the nanofibers were mounted on a brass stub using double-sided adhesive tape and sputtered with gold-palladium mixture for 1 h under vacuum using a Sputter Coater (Leica EM SCD005). The samples were analyzed using SEM under 5000x magnification. The average diameters of 100 nanofibers were measured at 5 different spots using ImageJ Software (ImageJ 1.52a).

Fourier-Transform Infrared Spectroscopy (FT-IR)

The chemical interactions between the crosslinking PC and GPC nanofiber samples were analyzed using Attenuated Total Reflectance-Fourier Transform Infrared Spectroscopy (ATR-FTIR, Perkin Elmer) to identify the presence of functional groups in the nanofibers. The ATR-FTIR spectra of the nanofiber samples were acquired at a spectral range of 600 – 4000 cm^{-1}.

Thermal Stability

The thermal properties of the nanofibers were analysed by thermogravimetric analysis (TGA, STA7200 Hitachi) using 4-5 mg nanofibers at a temperature range of 30 – 600°C at a heating rate of 10 °C/min under a nitrogen atmosphere.

In vitro Drug Release of Gentamicin Sulfate

The drug release of gentamicin was measured using a UV-Vis spectrophotometer (double beam) at λ_{max} = 201 nm [17]. The samples were cut into 2 x 2 cm squares, weighed and incubated in 20 mL distilled water at 37 °C. 4 mL of the soaking solution was analyzed using the UV-Vis Spectrophotometer at pre-determined time intervals up to 72 h to monitor the release rate with time [17]. The calibration curve ($y = 0.3865x - 0.0271$; $r^2 = 0.9985$) was constructed as a standard. The cumulative drug release was calculated using the following equation:

$$\frac{\text{Total amount of drug released from the membrane}}{\text{Total amount of drug present in the membrane}} \times 100\% \quad (1)$$

The encapsulation efficiency was calculated by the following equation,

$$\frac{\text{Weight of drug in the nanofibers}}{\text{Theoretical weight of drug in the nanofibers}} \times 100\% \quad (2)$$

The amount of drug in the membrane was determined using the following equation:

$$\frac{\text{Initial amount of drug loaded in the nanofibers}}{\text{Total weight of the nanofibers}} = \frac{\text{Theoretical amount of drug in the membrane}}{\text{Weight of the membrane}} \quad (3)$$

The kinetic release of gentamicin was investigated using zero-order, first order, Hixson-Crowell, Higuchi and Korsmeyer-Peppas models [18]. The *in vitro* gentamicin release followed the model with the highest linearity or correlation coefficient (r^2) value.

Zero-order model

The cumulative amount of drug released (Q_t) is plotted against time. The rate of drug release is independent of its concentration as shown below:

$$Q_t = k_1 t \quad (4)$$

where Q_t is the total drug release (in percentage concentration) at time, t and k_1 is the constant of the zero-order model (in concentration/time).

First-order model

The log of cumulative percentage of drug remaining is plotted against time. The rate of drug release is assumed to be dependent on its concentration as stated below:

$$Log_{10}\, Q_t - Log_{10}\, Q_0 = -\frac{k_2 t}{2.303} \quad (5)$$

where Q_0 is the initial concentration of the drug, k_2 is the constant of first-order model and t is time.

Hixson-Crowell model

Based on this model, the area of the particle is proportional to the cubic root of its volume. The drug release profile is described by considering the diminishing surface of the drug particle during dissolution as in the following equation:

$$Q_0^{1/3} - Q_t^{1/3} = k_3 t \quad (6)$$

where Q_0 is the initial concentration of the drug, Q_t is the amount of drug released at time t, and k_3 is the constant of the Hixson-Crowell model. A straight-line graph can be obtained by plotting ($Q_0^{1/3} - Q_t^{1/3}$) against t while the slope indicates the Hixson-Crowell constant.

Higuchi model

The equation below represents the simplified Higuchi model.

$$Q = k_4 t^{1/2} \quad (7)$$

where Q is the amount of drug released in time t, and k_4 is the Higuchi dissolution constant. The amount of drug released in the fixed timespans, represented as a function of the square root of time, fits a straight line.

Korsmeyer-Peppas model

The equation below represents the simplified Korsmeyer-Peppas model. The amount of drug released in the fixed timespans is represented on a log-log basis.

$$M_t/M = k_5\, t^n \quad (8)$$

where M_t and M are the amount of drug at time t, k_5 is the kinetic constant related to the delivery system while n is the release exponent that depends on the type of transport, geometry and polydispersity of the solute which illustrates the solute transport mechanism such that:

(1) $n < 0.5$ corresponds to a pseudo-Fickian diffusion

(2) $n = 0.5$ suggests Fickian behavior

(3) $0.5 < n < 1$ indicates an anomalous diffusion or non-Fickian transport

(4) $n = 1$ shows non-Fickian diffusion

***In vitro* Antibacterial Activity Assay**

The antibacterial activity of gentamicin sulfate-loaded PVA/Chitosan (GPC) nanofibers against *E. coli* (ATCC 25922) and *S. aureus* (ATCC 25923) was determined using a disc diffusion technique (Kirby Bauer method) in duplicate [19]. The bacteria were cultured using Mueller Hinton agar and broth for 24 h at 37.5 °C. PC and GPC nanofibers were cut into 5 mm diameter discs and place in each agar plate. The antibiotic disc with 10 µg of gentamicin was placed in the center of MH agar as a positive control. A blank paper disc was placed in each plate as a negative control. The plates were incubated at 37.5 °C for 24 hours. The bacteria inhibition zones were measured and compared on the 1st, 3rd and 5th days.

RESULTS AND DISCUSSION

Morphology of PC and GPC nanofibers

SEM images of PC and 1, 3 and 5% GPC electrospun nanofibers are presented in Figure 1. The PC (Figure 1a) nanofibers showed smooth non-woven nanofibers

without beads and broken strands but were irregular in size with an average fiber diameter of 228 ± 75 nm. To obtain smooth and homogeneous nanofibers, the solution parameters (concentration and solubility) and processing parameters (flow rate, viscosity and voltage supply) need to be optimized [20]. The incorporation of 1-5% gentamicin sulfate in PC solution increased the diameter of the fibers and several defects can be observed due to higher drug loading into the nanofibers. In Figure 1(b)-(d), 1% GPC showed smooth and bead-free nanofibers with a smaller average diameter of 288 ± 114 nm. As the GS concentration was increased up to 3%, the diameter increased to 332 ± 87 nm and there were beads observed due to the irregularly dissolved drug in the polymer solution [21].

When the concentration of GS was increased to 5%, the solution turned cloudier and the Taylor's cone formed was unstable due to the higher drug concentrations, leading to the formation of droplets and beaded nanofibers with a larger diameter [22]. Therefore, the addition of 5 % GS in PC solution results in the formation of larger diameter nanofibers (354 ± 113 nm). This may be due to the formation of intermolecular hydrogen bonding, Van der Waals forces and dipole-dipole interactions between GS, PVA and Chitosan molecules [18]. Since PVA is a water-soluble polymer and easily degraded in water, crosslinking of the nanofibers is necessary to slow down its degradation [23].

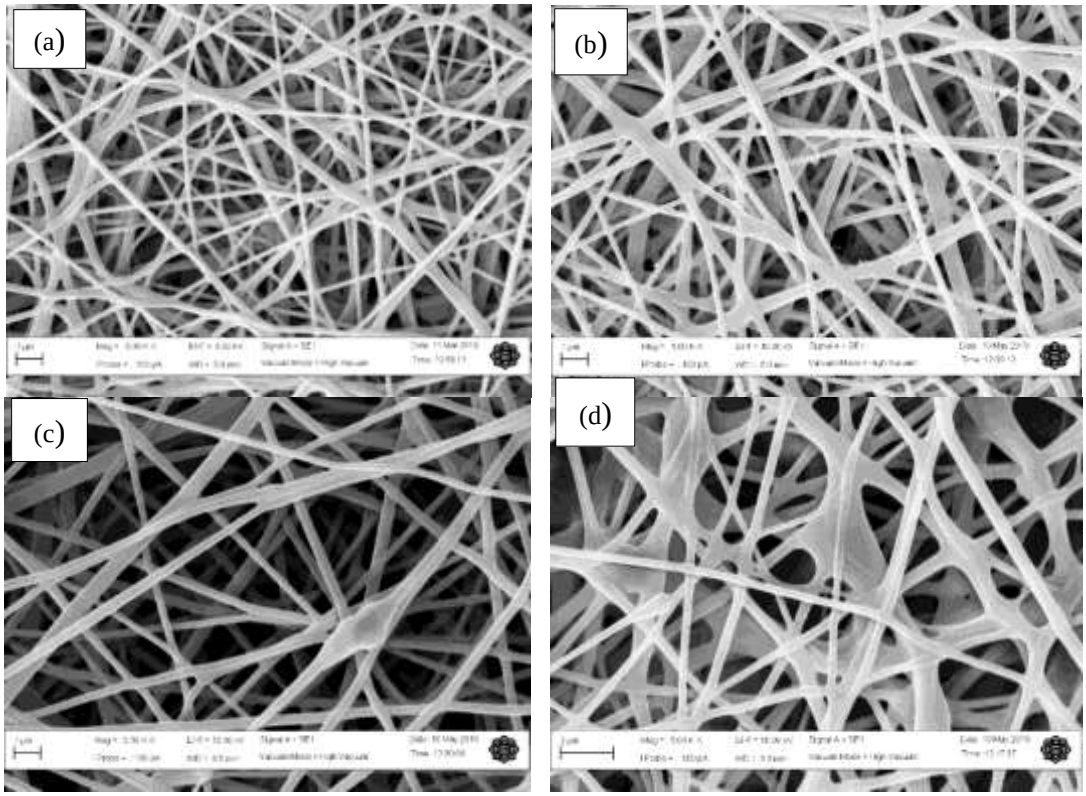

Figure 1. SEM images of (a) PC, (b) 1GPC, (c) 3GPC and (d) 5GPC nanofibers. (5000x magnification)

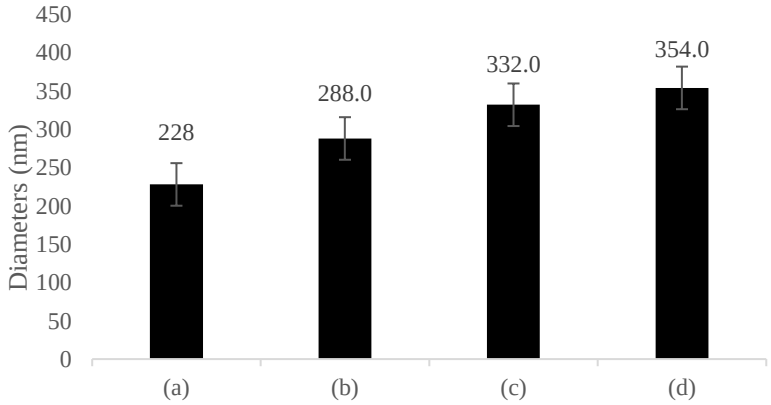

Figure 2. Fiber diameters of (a) PC, (b) 1GPC (c) 3GPC (d) 5GPC nanofibers

ATR-FTIR Spectroscopy

Figure 3 shows the ATR-FTIR spectra of crosslinking PC and GPC electrospun nanofibers. The characteristic bands of non-crosslinking PC (Figure 3(a)) include the broad peak at 3295 cm^{-1} caused by the O-H stretching bond from the hydroxyl group of PVA [17]. The peak at 2914 cm^{-1} is due to asymmetric C-H stretching of the methyl group. The presence of chitosan in the PC nanofibers was indicated by a sharp peak at 1715 cm^{-1} which belongs to the C=O stretching of the carbonyl group of the remaining vinyl acetate repeat units in the PVA, as PVA is produced by copolymerization of vinyl alcohol and vinyl acetate repeat units [24,25]. The small peak at 1561 cm^{-1} was assigned to NH-bending of the amide group in chitosan and the peak at 1025 cm^{-1} to the C-O aryl stretch. The crosslinking of the PC nanofibers (Figure 3(b)) increased the intensity of the O-H group and C=O group peaks. This indicates the presence of glutaraldehyde (GA) crosslinking, which might prevent the nanofibers from absorbing surrounding water and moisture [23].

Similarly, the peaks that appeared in crosslinking PC nanofibers were also present in the crosslinking GPC spectra (Figure 3c-3e). It can be observed from this figure that the intensity of the carbonyl stretching peak at 1715 cm^{-1} increased when gentamicin is added into the nanofibers as a result of intermolecular hydrogen bond interactions between GS and PC molecules (Figure 4). In addition, the peak of the C-O stretch in PC shifted to 1055 cm^{-1}, indicating the presence of the C-O aryl group from gentamicin in the nanofibers. As the concentration of gentamicin was increased, the intensity of the peaks also increased, confirming that gentamicin was successfully encapsulated into the nanofibers.

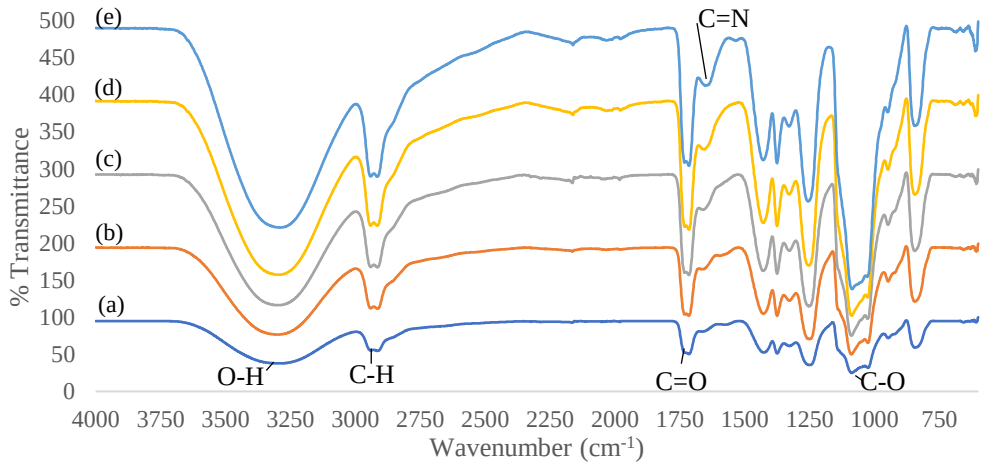

Figure 3. ATR-FTIR spectra of (a) non-crosslinking PC, (b) crosslinking PC, (c) crosslinking 1GPC, (d) crosslinking 3GPC and (e) crosslinking 5GPC nanofibers respectively.

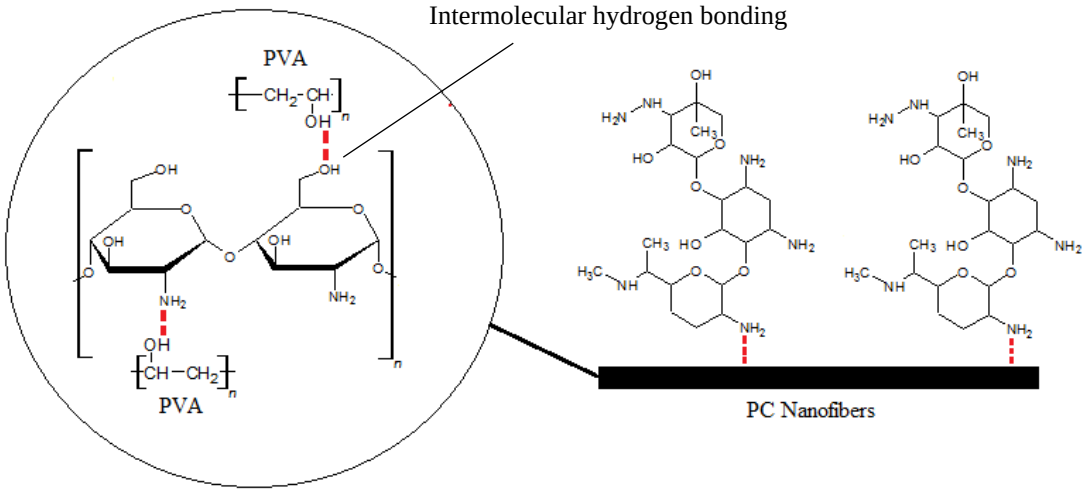

Figure 4. Schematic illustration of the possible formation of intermolecular hydrogen bonds in the blending of PC and GPC nanofibers [26,27].

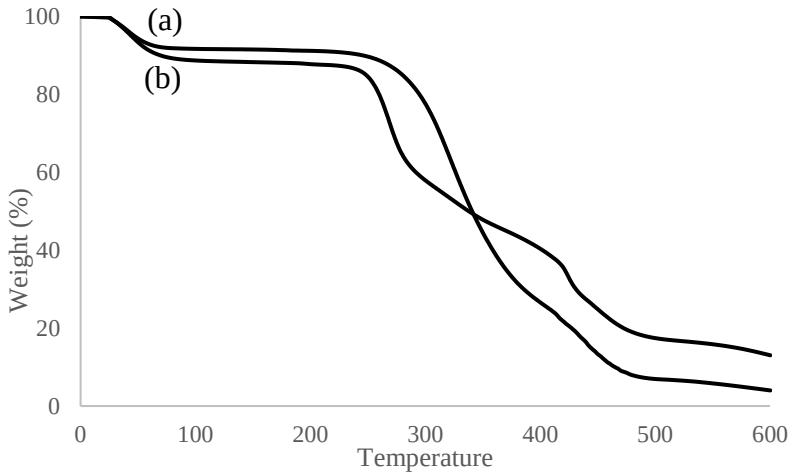

Figure 5. TGA weight loss of crosslinked nanofibers (a) PC (b) GPC

Thermal Stability

TGA analysis was performed to examine the thermal stability of both PC and GPC crosslinked nanofibers (Figure 5). The TGA curve indicates that thermal degradation of these nanofibers happened at three stages: 30-60, 230-350 and 400-500 °C. The initial weight loss (below 100 °C) was due to the loss of volatile components such as moisture via evaporation [28]. A significant decomposition of the PC and GPC nanofibers started at 284 °C (a weight loss of 65.89%) and 249 °C (a weight loss of 43.1%) respectively. The significant weight loss continued up to 429 °C (a weight loss of 84.75%) for PC nanofibers and to 413 °C for GPC nanofibers (a weight loss of 71.55 %). The degradation of both nanofibers was almost complete at 544 and 567 °C respectively, with a slight amount (0.52% of PC and 6.54% of GPC) remaining undecomposed. The addition of gentamicin to PC nanofibers reduced the thermal stability of the PC nanofibers (Figure 4a and 4b). The decrease in thermal stability might be related to the morphological change in PC [28] due to the addition of gentamicin as shown in the SEM results (Figure 1(a-d)). The addition of gentamicin sulfate further increased the surface area of PC nanofibers, providing a greater area for water adsorption [29]. In addition, gentamicin sulfate powder is hygroscopic in nature. Hence, it increases the water content adsorbed on the nanofibers and reduces its thermal stability [30].

***In vitro* Drug Release Study**

The drug encapsulation efficiencies are recorded in Figure 6(a). The higher the concentration of gentamicin loaded in the PC nanofibers, the higher the encapsulation efficiency. This may be attributed to the increased intermolecular hydrogen bonding between gentamicin and PVA/chitosan as the drug carrier [26,27]. Gentamicin in the nanofibers showed an initial burst release effect for the first 12 hours, followed by sustained release at a slower rate up to 72 hours. 1 % GPC showed a higher cumulative release rate of about 70 % compared to 3 % and 5 % GPC (Figure 6(b)) which had release rates of about 26 % and 14 % respectively. This might be due to the higher

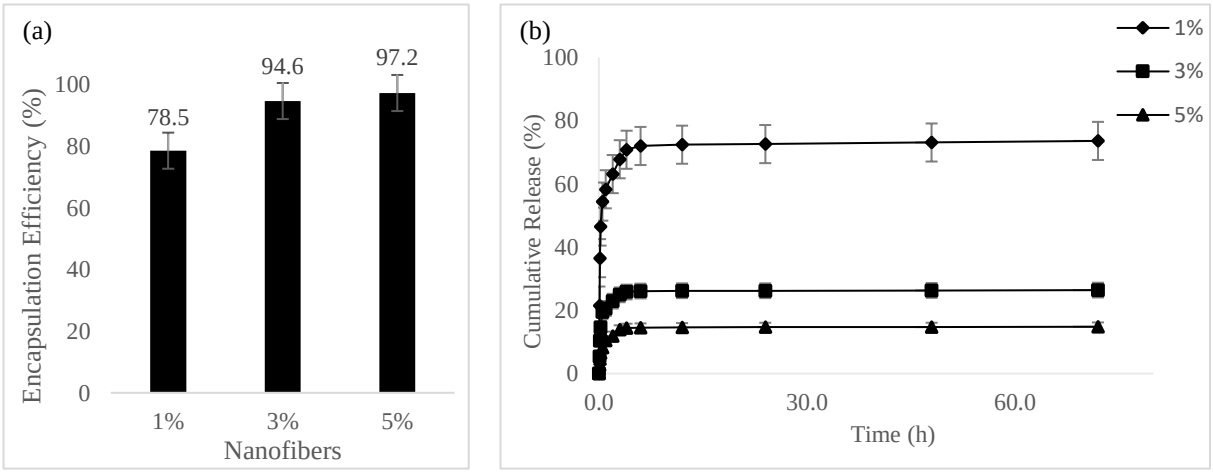

Figure 6. (a) Encapsulation efficiency of 1, 3 and 5 % GPC nanofibers, (b) Cumulative drug release of 1, 3 and 5 % GPC nanofibers.

encapsulation efficiency (Figure 6(a)) of gentamicin in 3 % and 5 % GPC, where the drug is mainly confined in the nanofibers [17], and thus has difficulty separating from the nanofibers due to the strong intermolecular hydrogen bonding between GS and PVA. In addition, the smaller the diameter of the nanofibers, the higher the drug release rate.

From observation, the PC solution became cloudy as the concentration of GS loaded was increased. This indicates that the undissolved gentamicin was being suspended in the polymer fiber matrix. In the case where undissolved drug particulates were suspended in the polymer fiber matrix, the drug is distributed in the polymer matrix as crystalline or amorphous particles [21]. The drug is initially dissolved and embedded in the surrounding polymer fiber matrix. The dissolved drug reaches the surface layer of the nanofibers by diffusion and attaches itself to the aqueous boundary layer of the nanofibers interface. The drug molecules are then delivered through diffusion across the boundary layer into the aqueous medium (as illustrated in Figure 7). As gentamicin has a low solubility and is not completely miscible in PVA and chitosan solution, it showed an unexpectedly high initial rate of release (usually referred to as burst release) [21]. Another alternative to improve the miscibility of gentamicin with PVA and chitosan is by chemically modifying the polymer backbone or adding molecules that consists of both hydrophobic and hydrophilic moieties (i.e. surfactant) [31]. The diameter of the nanofibers and the drug's physical properties such as solubility and drug-polymer interactions may significantly affect the drug release rate [28].

The cumulative release data were fitted into five mathematical kinetic release models (zero-order, first-order, Hixson-Crowell, Higuchi and Korsmeyer-Peppas models) to observe and understand the mechanism of drug release. The correlation coefficients, r^2, are tabulated in Table 1.

In vitro release of crosslinked GPC nanofibers showed the best linearity in the Korsmeyer-Peppas model as it shows the highest correlation coefficient. The Korsmeyer-Peppas slope exponent (n) was less than 0.5 which confirmed that the release mechanism of GS followed the pseudo-Fickian diffusion mechanism for both nanofibers. This indicates that the gentamicin release mechanism is due to the kinetic degradation and erosion of the polymer matrix via hydrolysis [25]. The erosion of nanofibers happens in three stages: Firstly, the drug is released from the polymer surfaces or pores. Then, a little polymer degradation occurs causing the remaining drug to be trapped in the matrix. Lastly, the trapped drug is released rapidly when the polymer chains disintegrate. However, it is possible for the polymer system to leave the site before the drug is completely released due to very slow erosion [29].

In vitro Antibacterial Activity Assay

The antimicrobial activity of gentamicin released from crosslinked PC nanofibers was estimated by measuring the diameter of the bacterial inhibition zones for 1, 3 and 5 days. Figure 8 shows the antibacterial activity of GPC nanofibers against *E. col*i and *S. aureus* bacteria. The inhibition zones of GPC nanofibers were larger than the positive control. This is because chitosan used in the formulation also has antibacterial properties [30], which further enhances the antibacterial activity. The GPC nanofibers showed a better antibacterial activity against both bacteria. For *E. coli* (Figure 8(a-b)), the higher the concentration of GS loaded, the greater the diameters of the inhibition zones observed. In addition, the diameters of the

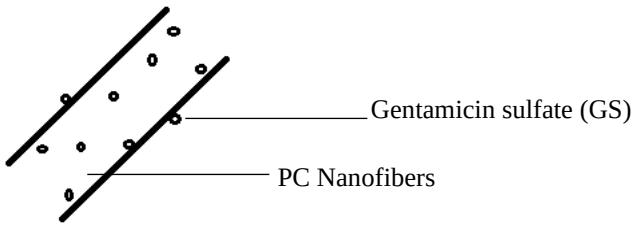

Figure 7. Illustration of gentamicin dissolution in PC nanofibers

Table 1. Comparison of kinetic release models for crosslinked GPC nanofibers.

Nanofibers	r^2					
	Zero order	First order	Hixson-Crowell	Higuchi	Korsmeyer-Peppas	n
1 % GS	0.2069	0.1782	0.1987	0.4027	0.7019	0.1399
3 % GS	0.2056	0.1540	0.1743	0.4069	0.6672	0.1796
5 % GS	0.2498	0.1942	0.2159	0.4742	0.7613	0.2156

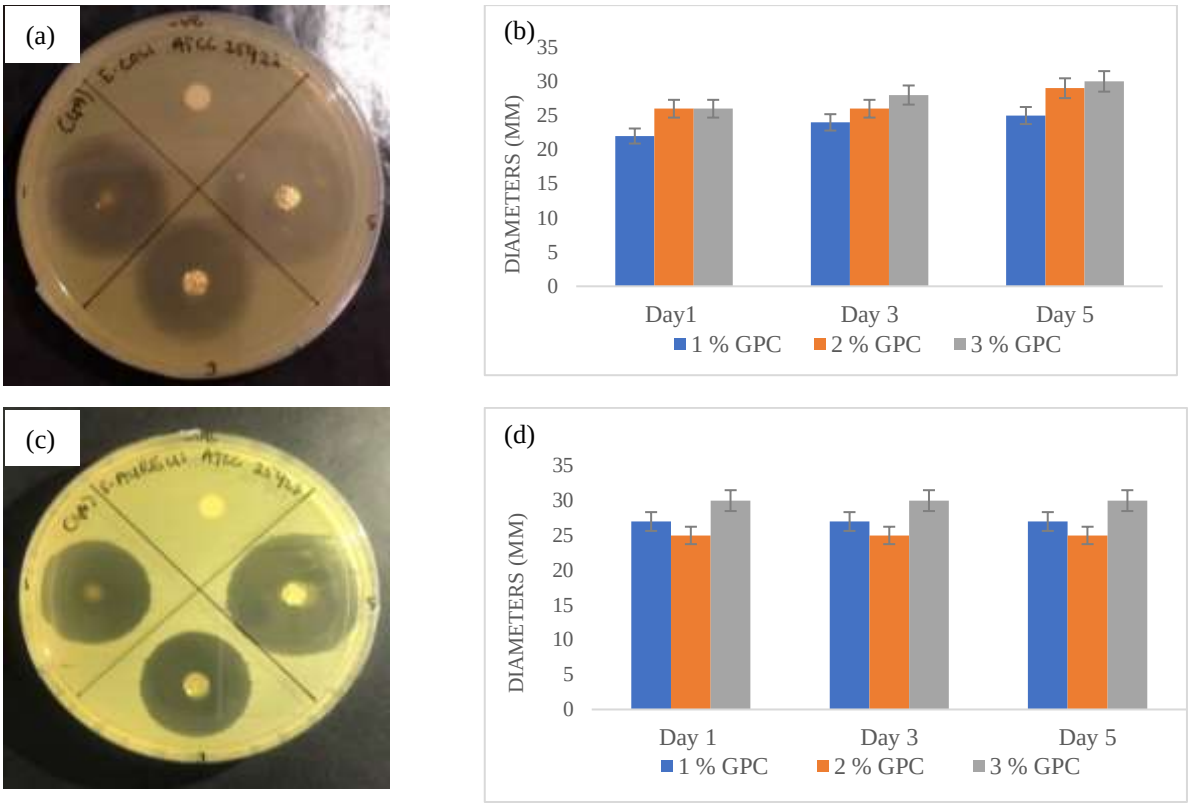

Figure 8. (a) Inhibition zones of GPC nanofibers against *E. coli*, (b) Average diameters of *E. coli* inhibition zones over 5 consecutive days, (c) Inhibition zones of GPC nanofibers against *S. aureus*, (d) Average diameters of *S. aureus* inhibition zones over 5 consecutive days.

bacteria inhibition zones increased by 1 to 2 mm from day 1 to day 5. On the other hand, the 5 % GPC showed the highest inhibition zone diameters for *S. aureus* while 3 % GPC showed the smallest bacteria inhibition zones (Figure 8(c-d)). This might be due to the irregular dissolution of the drug in the nanofibers. Further work in this area should include analysis in triplicate or more to achieve higher accuracy on the inhibition zone measurements.

CONCLUSION

Crosslinked PC nanofibers loaded with gentamicin sulfate at different concentrations were successfully fabricated using an electrospinning technique. Fine nanoscale fibers with a diameter of approximately 288 nm to 354 nm were obtained. ATR-FTIR confirmed the presence of gentamicin sulfate molecules encapsulated in the network of PC nanofibers. The thermal stability of PC nanofibers decreased with the addition of gentamicin sulfate. The *in vitro* drug release profile revealed that PC has great potential as a drug carrier as it can provide a sustained release of gentamicin sulfate for up to 72 hours. The kinetic drug release followed the Korsmeyer-Peppas model with release exponent, $n < 0.5$. The fabricated nanofibers successfully inhibited the growth of Gram-negative (*E. coli*) and Gram-positive *(S. aureus*) bacteria. In conclusion, crosslinked PC loaded with gentamicin sulfate shows a promising future as an excellent drug delivery system for controlled release of hydrophilic drugs. The data obtained in this study can be used to further optimize drug loading and drug release capacity for effective targeted application.

ACKNOWLEDGMENT

This work was supported by the IIUM Research Acculturation Grant Scheme (IRAGS18-033-0034).

REFERENCES

1. Zafar, M., Najeeb, S., Khurshid, Z., Vazirzadeh, M., Zohaib, S. & Najeeb, B. (2016) Potential of electrospun nanofibers for biomedical and dental applications. *Materials (Basel)*, **9(2)**,1–21.

2. Gaaz, T. S., Sulong, A. B., Akhtar, M. N., Kadhum, A. A., Mohamad, A. B. and Al-Amiery, A. A. (2015) Properties and Applications of Polyvinyl Alcohol, Halloysite Nanotubes and Their Nanocomposites. *Molecules*, **20(12)**, 22833–22847.

3. Akduman, C., Morsunbul, S., Widiyandari, H. and Purwanto, A. (2018) Stabilization of PVA / Chitosan / TiO 2 Nanofiber Membrane with Heat Treatment and Glutaraldehyde. *IOP Conf.*

Mater. Sci. Eng., **367**.

4. Wang, J. and Ye, L. (2014) Structure and properties of polyvinyl alcohol/polyurethane blends. *Compos Part B Eng.*, **69(3)**, 89–96.

5. Kimbonguila, A., Matos, L., Petit, J., Scher, J. and Nzikou, J. M. (2019) Effect of Physical Treatment on the Physicochemical, Rheological and Functional Properties of Yam Meal of the Cultivar "Ngumvu" From Dioscorea Alata L. of Congo. *Int. J. Recent Sci. Res.*, **8(3)**, 15773–15776.

6. Steyaert, I., Van Der Schueren, L., Rahier, H. and De Clerck, K. (2012) An alternative solvent system for blend electrospinning of polycaprolactone/chitosan nanofibres. *Macromol. Symp.*, **321–322(1)**, 71–75.

7. Jin, R. M., Sultana, N., Baba, S., Hamdan, S. and Ismail, A. F. (2015) Porous PCL/Chitosan and nHA/PCL/chitosan scaffolds for tissue engineering applications: Fabrication and evaluation. *J. Nanomater.*, **2015**.

8. Sandri, G., Bonferoni, M. C., Ferrari, F., Rossi, S., Aguzzi, C. and Mori, M. (2014) Montmorillonite-chitosan-silver sulfadiazine nanocomposites for topical treatment of chronic skin lesions: In vitro biocompatibility, antibacterial efficacy and gap closure cell motility properties. *Carbohydr. Polym.*, **102(1)**, 970–977.

9. Xia, G., Lang, X., Kong, M., Cheng, X., Liu, Y. and Feng, C. (2016) Surface fluid-swellable chitosan fiber as the wound dressing material. *Carbohydr. Polym.*, **136**, 860–866.

10. Naseri-Nosar, M. and Ziora, Z. M. (2018) Wound dressings from naturally-occurring polymers: A review on homopolysaccharide-based composites. *Carbohydr. Polyms.*, **189**, 379–398.

11. Gautam, S., Chou, C. F., Dinda, A. K., Potdar, P. D. and Mishra, N. C. (2014) Fabrication and characterization of PCL/gelatin/chitosan ternary nanofibrous composite scaffold for tissue engineering applications. *J. Mater. Sci.*, **49(3)**, 1076–1089.

12. Alhosseini, N. S., Moztarzadeh, F., Mozafari, M., Asgari, S., Dodel, M. and Samadikuchaksaraei, A. (2012) Synthesis and characterization of electrospun polyvinyl alcohol nanofibrous scaffolds modified by blending with chitosan for neural tissue engineering. *Int. J Nanomedicine*, **7**, 25.

13. Abraham. A., Soloman. P. A. and Rejini. V. O. Preparation of Chitosan-Polyvinyl Alcohol Blends and Studies on Thermal and Mechanical Properties. *Procedia Technol.*, **24**, 741–748.

14. El-Hefian, E. A., Nasef, M. M. and Yahaya, A. H. (2010) The preparation and characterization of Chitosan/Poly (Vinyl Alcohol) blended films. *E-Journal Chem.*, **7(4)**, 1212–1219.

15. Gonçalves, R. P., Ferreira, W. H., Gouvêa, R. F. and Andrade, C. T. (2017) Effect of Chitosan on the Properties of Electrospun Fibers From Mixed Poly(Vinyl Alcohol)/Chitosan Solutions. *Mater. Res.*, **20(4)**, 984–993.

16. Rezaee, S. and Moghbeli, M. R. (2014) Crosslinked Electrospun Poly (Vinyl Alcohol) Nanofibers Coated by Antibacterial Copper Nanoparticles. *Iran. J Chem. Eng.*, **11(3)**, 45–58.

17. Abdul Khodir, W., Abdul Razak, A., Ng, M., Guarino, V. and Susanti, D. (2018) Encapsulation and Characterization of Gentamicin Sulfate in the Collagen Added Electrospun Nanofibers for Skin Regeneration. *J. Funct. Biomater.*, **9(2)**, 36.

18. Sriyanti, I., Edikresnha, D., Rahma, A., Miftahul Munir, M., Rachmawati, H. and Khairurrijal, K. (2018) Mangosteen pericarp extract embedded in electrospun PVP nanofiber mats: physicochemical properties and release mechanism of α-mangostin. *Int. J. Nanomedicine.*, **13**, 4927–4941.

19. Coimbra, P., Freitas, J. P., Gonçalves, T., Gil, M. H. and Figueiredo, M. (2019) Preparation of gentamicin sulfate eluting fiber mats by emulsion and by suspension electrospinning. *Mater. Sci. Eng. C.*, **94**, 86–93.

20. Robb, B. and Lennox, B. (2011) The electrospinning process, conditions and control. Electrospinning Tissue Regen. **51–66**.

21. Andrady, A. L. (2008) Biomedical applications of nanofibers. *John Wiley & Sons, Inc.*, **183–223.**

22. Qasim, S. B, Zafar, M. S., Najeeb, S., Khurshid, Z., Shah, A. H. and Husain, S. (2018) Electrospinning of chitosan-based solutions for tissue engineering and regenerative medicine. *Int. J. Mol. Sci.*, **19(2)**, 407.

23. Pouranvari, S., Ebrahimi, F., Javadi, G. and Maddah, B. (2016) Chemical cross-linking of chitosan/polyvinyl alcohol electrospun nanofibers. *Mater. Technol.*, **50(5)**, 663–666.

24. Cui, Z., Zheng, Z., Lin, L., Si, J., Wang, Q. and Peng, X. (2018) Electrospinning and crosslinking of polyvinyl alcohol/chitosan composite nanofiber for transdermal drug delivery. *Adv. Polym. Technol.*, **37(6)**, 1917–1928.

25. Mozafari, M., Moztarzadeh, Jalali, Alhosseini, N., Asgari and Dodel (2012) Synthesis and characterization of electrospun polyvinyl alcohol nanofibrous scaffolds modified by blending with chitosan for neural tissue engineering. *Int. J. Nanomedicine*, **7**, 25**–**34.

26. Kadhim, I. A., Zubaidi, A. B. A., Alameer, Z. J. A, Hameed, F. M. and Sadeq, A. W. (2020) Genipin cross-linked chitosan/polyvinyl alcohol blend for biomedical engineering. Indian J. Forensic Med. *Toxicol*., **14(3)**, 1625–1631.

27. Chung, T., Park, J., Lee, H., Kwon, H., Kim, H. and Id, Y. L. (2018) The improvement of mechanical properties, thermal stability, and water absorption resistance of an eco- friendly PLA/Kenaf biocomposite using acetylation. *Appl. Sci*., **8**, 376.

28. Kharaghani, D., Gitigard, P., Ohtani, H., Kim, K. O. and Ullah, S. (2019) Design and characterization of dual drug delivery based on in-situ assembled PVA/PAN core-shell nanofibers for wound dressing application. *Sci. Rep.*, **9**, 12640.

29. Stevanovi, M., Jankovic, A., Koji, V., Vukašinovi, M., Odovi, J. and Saka, M. C. (2018) Gentamicin-loaded bioactive hydroxyapatite/chitosan composite coating electrodeposited on titanium. *ACS Biomater. Sci. Eng.*, **4(12)**, 3994**–**4007.

30. Zhou, H., Liu, X., Wu, F., Zhang, J., Wu, Z., Yin, H. and Shi, H. (2016) Preparation, Characterization, and Antitumor Evaluation of Electrospun Resveratrol Loaded Nanofibers. *J Nanomater*., **2016**, 1**–**11.

31. Brianezi, S. F. S., Castro, K. C., Piazza, R. D., Melo, M., Do, S. F., Pereira, R. M. and Marques, R. F. C. (2018) Preparation and characterization of Chitosan/MPEG-PCL blended membranes for wound dressing and controlled gentamicin release. *Mater Res.*, **21(6),** 20170951.